Supplement of Biogeosciences, 17, 1955–1973, 2020
https://doi.org/10.5194/bg-17-1955-2020-supplement

Biogeosciences Open Access EGU

Supplement of

Vivianite formation in ferruginous sediments from Lake Towuti, Indonesia

Aurèle Vuillemin et al.

Correspondence to: Aurèle Vuillemin (a.vuillemin@lrz.uni-muenchen.de)

sample	dissolution procedure	δ^{56}Fe	sediment depth (m)
vivianite			
9H3	2M nitric acid, 24h	-0.44	23.4
9H3	2M nitric acid, 24h	-0.52	23.4
15A3	2M nitric acid, 24h	-0.61	36.7
21A1	2M nitric acid, 24h	-0.46	46.8
21A1	2M nitric acid, 24h replicate[a]	-0.39	46.8
reference			**2 standard mean deviation**
HanFe	pure Fe solution - not processed	0.31	± 0.02 (n=10)
BHVO-2	10% acet. acid/24h, then HF/HNO_3	-0.12	± 0.01 (n=2)
COQ-1	10% acet. acid/24h, then HF/HNO_3	-0.05	± 0.04 (n=2)
COQ-1	6M HCl/24h, then HF/HNO_3	-0.02	± 0.04 (n=4)
COQ-1	HCl/HF/HNO_3 total digestion	-0.04	± 0.04 (n=4)
literature			
HanFe	pure Fe solution - not processed	0.29	Moeller et al. (2014)
COQ-1	total digestion	-0.12	Craddock and Dauphas (2011)
COQ-1	total digestion	0.00	Dideriksen et al. (2006)
COQ-1	total digestion	0.07	Dideriksen et al. (2006)
COQ-1	total digestion	-0.07	He et al. (2015)
BHVO-2	total digestion	0.11	Craddock and Dauphas (2011)

The uncertainty in the Fe isotope data is 0.05 ‰ (2SD,δ^{56}Fe).

[a]Full procedure replicate incl. sample dissolution of a different crystal (vivianite), Fe column chemistry purification and measurement by MC-ICP-MS.

Supplementary Table S1:Results of data quality control for iron isotopes. Measurement accuracy and precision was assessed by repeated analyses of pure Fe standard solution (HanFe) and reference material COQ-1 and BHVO-2. Results for HanFe are identical to those obtained in an inter-laboratory comparison (Moeller et al., 2014). Those for COQ-1 and BHVO-2 are in agreement with published results within uncertainty limits.

References

Craddock, P.R., and N. Dauphas. 2011. Iron isotopic compositions of geological reference materials and chondrites. Geostand. Geoanal. Res. 35: 101-123.

Dideriksen, K., J.A. Baker, and S.L.S. Stipp. 2006. Iron isotopes in natural carbonate minerals determined by MC-ICP-MS with a Fe-58-Fe-54 double spike. Geochim. Cosmochim. Ac. 70: 118-132.

He, Y.S., S. Ke, F.Z. Teng, T.T. Wang, H.J. Wu, Y.H. Lu, and S.G. Li. 2015. High-precision iron isotope analysis of geological reference materials by high-resolution MC-ICP-MS. Geostand. Geoanal. Res. 39: 341-356.

Moeller, K., R. Schoenberg, T. Grenne, I.H. Thorseth, K. Drost, and R.B. Pedersen. 2014. Comparison of iron isotope variations in modern and Ordovician siliceous Fe oxyhydroxide deposits. *G*eochim. Cosmochim. Ac. 126: 422-440.

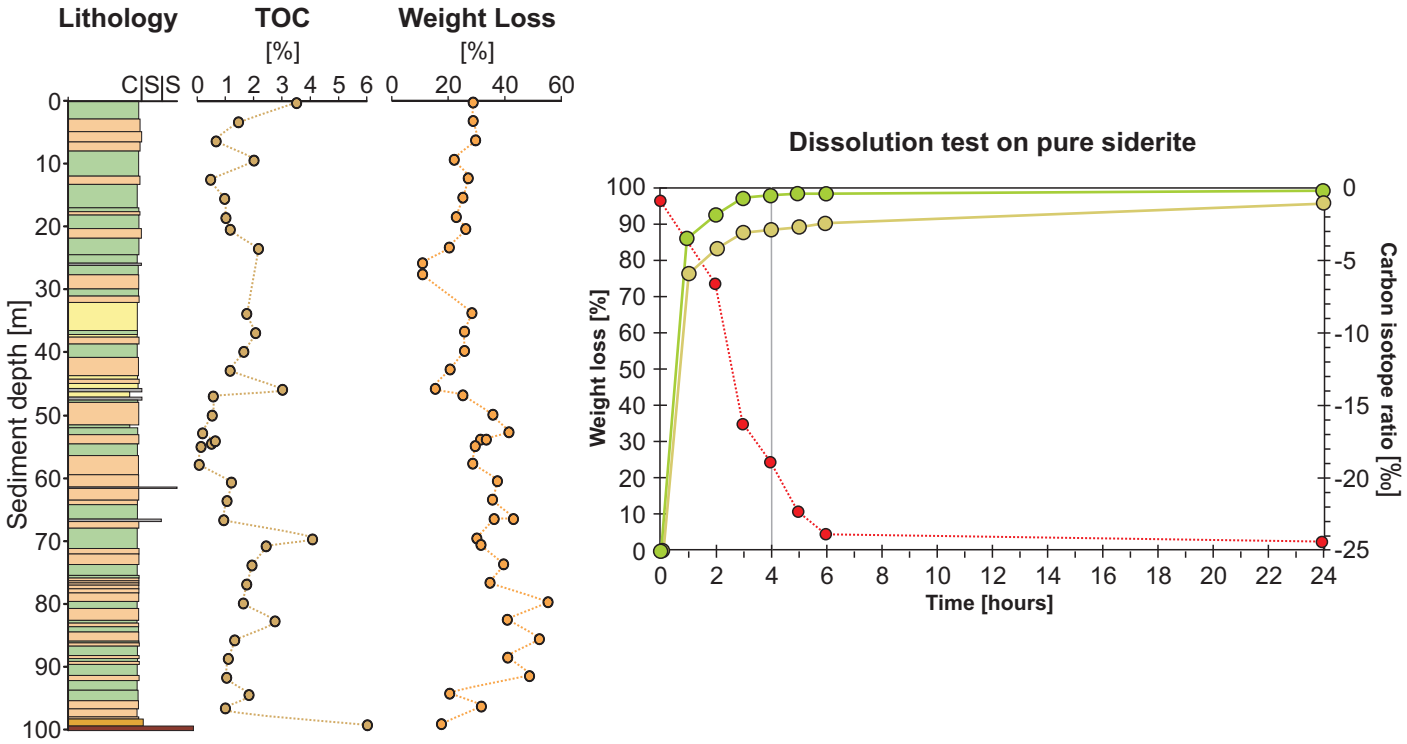

Supplementary Figure S1: Treatment of bulk sediments and siderite for carbonate dissolution. Bulk sediment samples were treated with 20 mL of 5 % HCl at 50° C for 24 hours to remove carbonates. This treatment was tested with 200 mg of technical grade siderite to evaluate its dissolution over time. Results show that 85 to 95 % of the siderite weight is dissolved after 2 hours. After 24 hours, >95% of siderite is dissolved, ensuring accurate measurement of both total organic carbon content and $\delta^{13}C$ composition on bulk sediment.

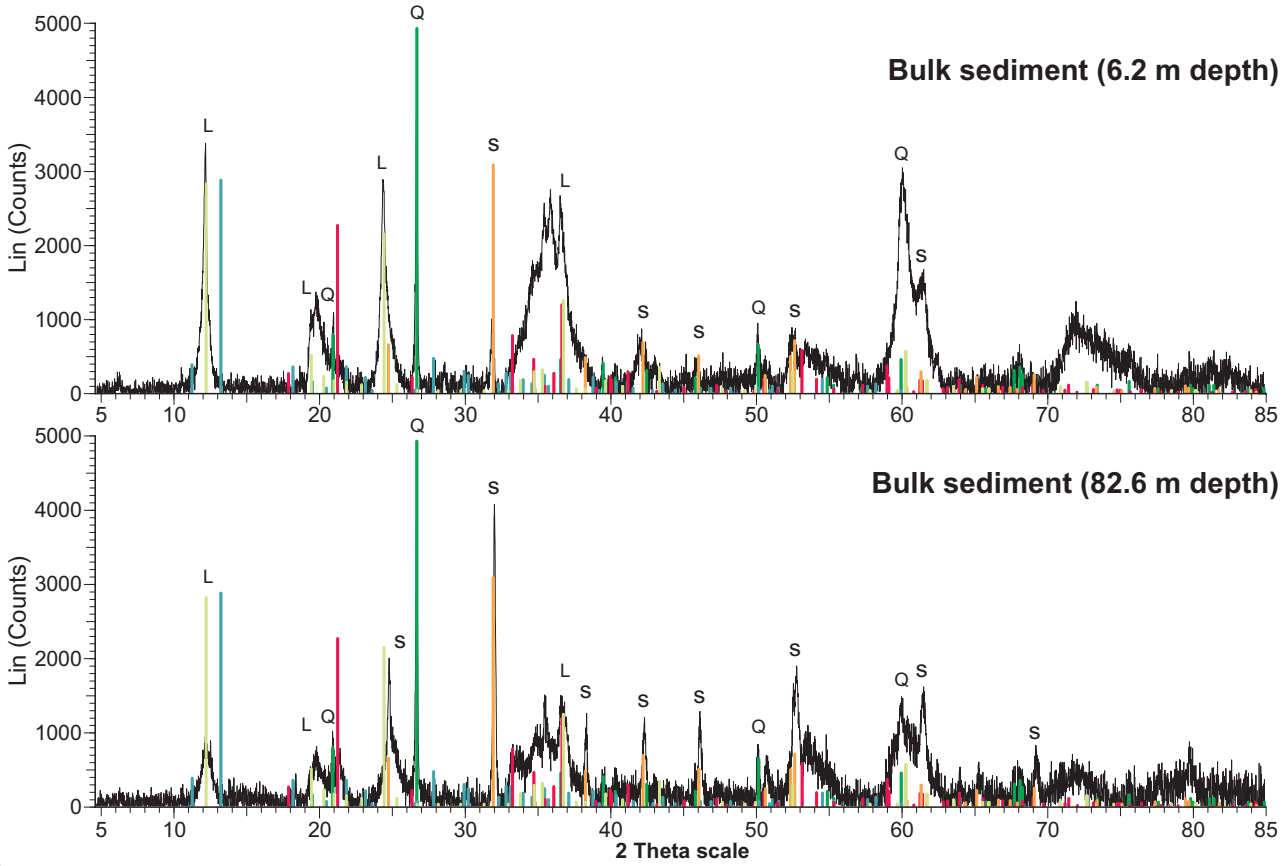

Supplementary Figure S2: Interpretations of XRD patterns for bulk sediments. Bulk sediment samples were selected at 6 different depth (6.3, 12.4, 23.4, 52.7, 66.5, and 82.6 m depth). Background substraction was applied to correct for the high iron content (>20 % wt). Peaks specific to siderite are clearly identified in the two spectra presented here, whereas vivianite is not present or accounts for less than 3% of the mineral fraction. Quartz and lizardite (i.e. serpentine) are clearly identified, whereas the broad peaks correspond to multiple iron-bearing phases and require focused XRD scans to be resolved. This data show that vivianite does not occur in bulk sediment outside the studied interval.

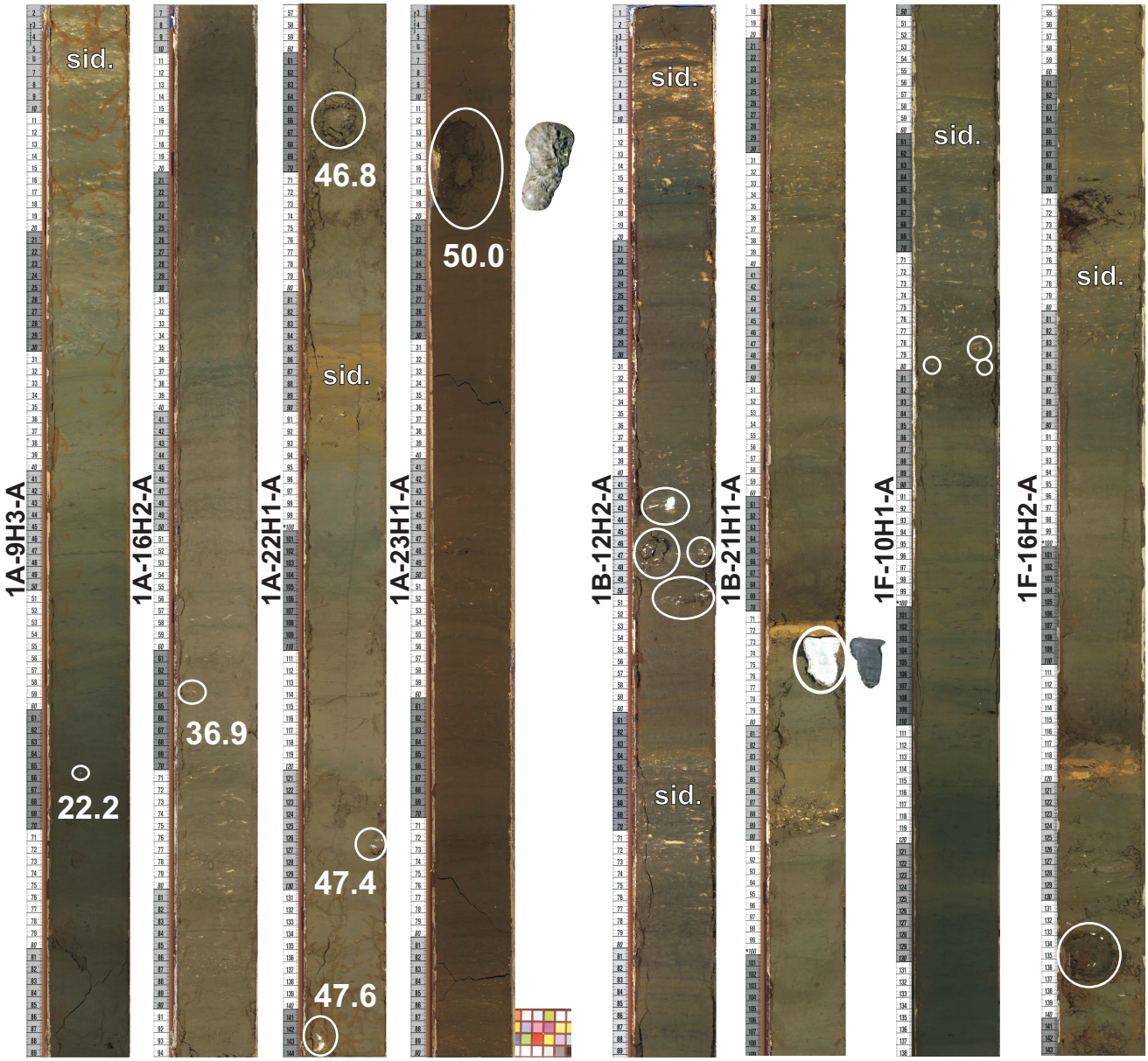

Supplementary Figure S3: Core scanning images for sections in which vivianite was identified. Sediments display variations in colors from light to dark brown with grey-green transitions, presently interpreted as reflecting redox conditions at the water-sediment interface. In the record of site 1A (left), vivianites are usually found in the darker layers. However at site 1B, vivianite crystals are also found close to sideritic beds.

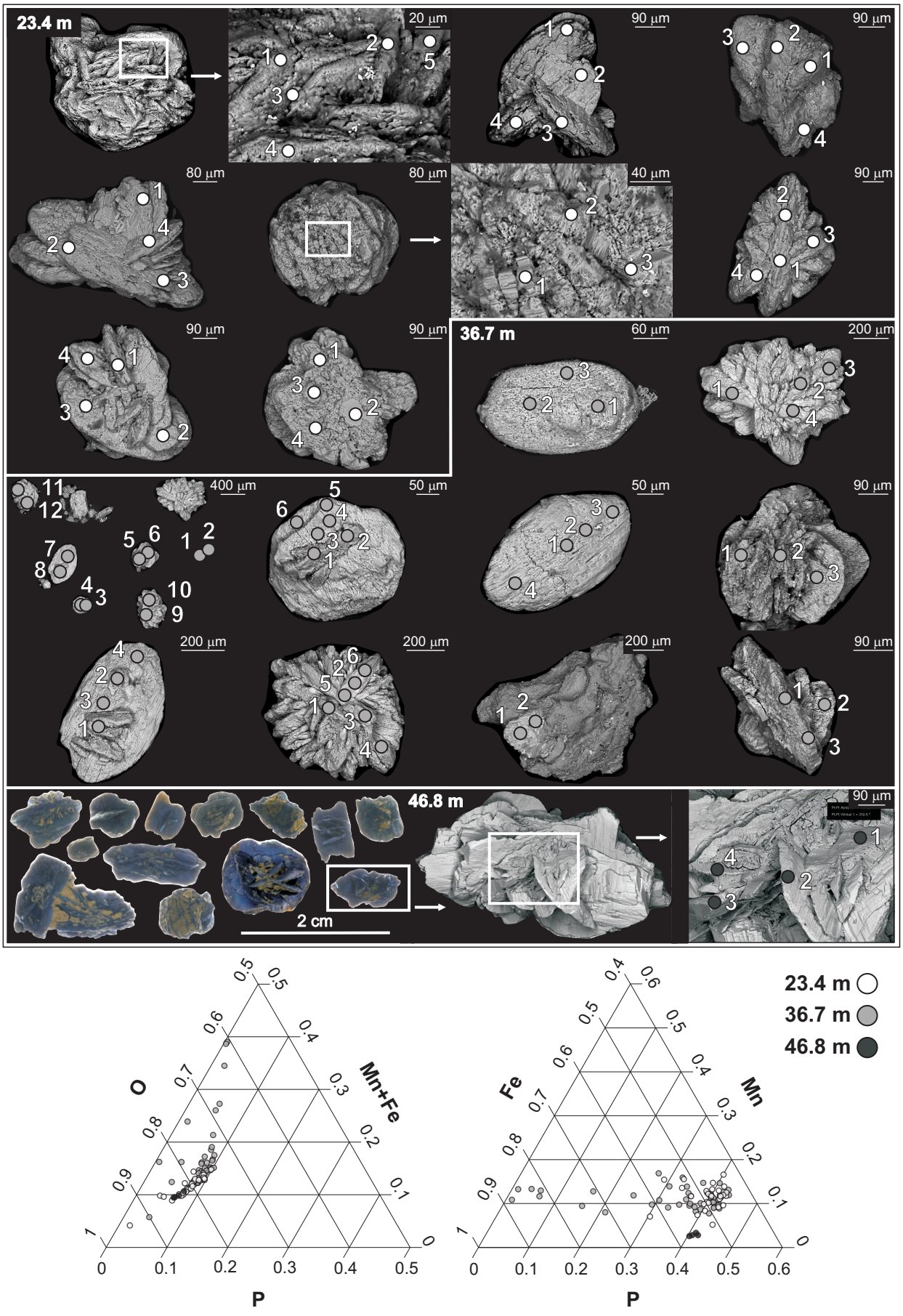

Supplementary Figure S4: SEM images with location of EDX points of analysis. SEM images in back-scattering electron mode (BSE) show that the habitus of vivianite evolves from tabular to rosette by the addition of blades. The different dots on the images signify points of EDX analysis. Results plotted in the two ternary diagrams below indicate an overall manganoan composition of the vivianites close to stoichiometric values.

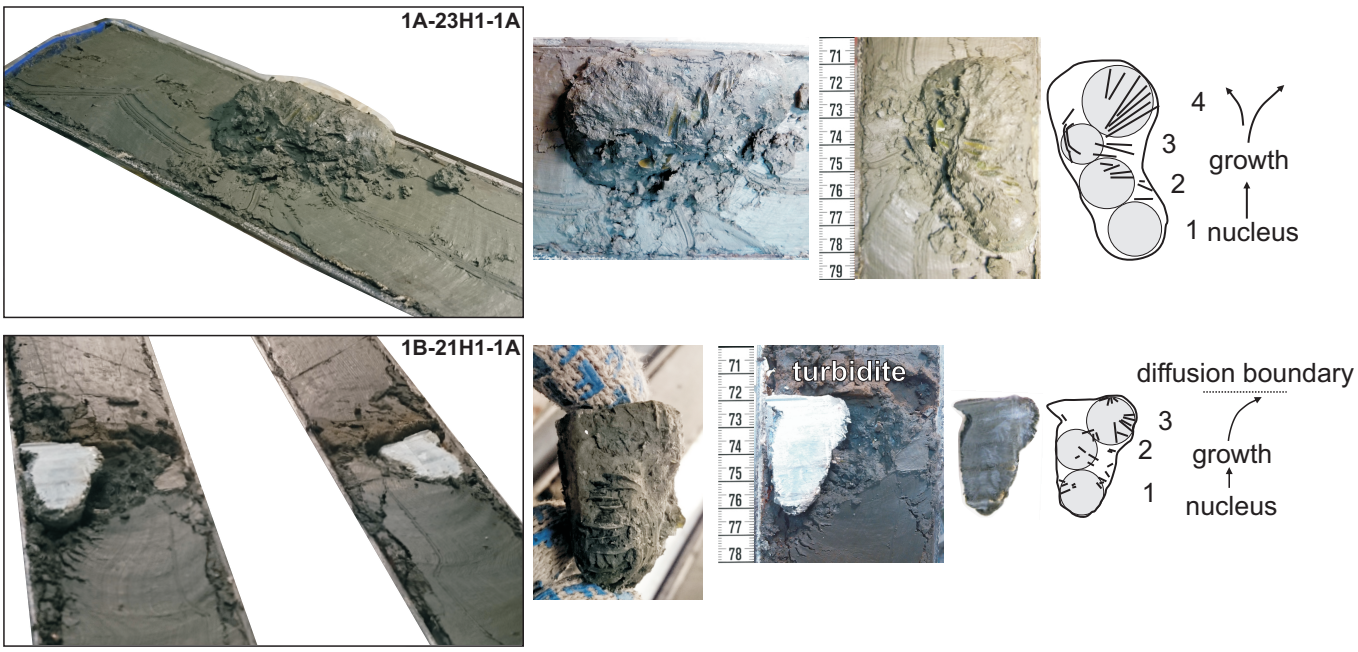

Supplementary Figure S5: Vivianite images taken on open cores and description of growth. The largest observed vivianite crystals were up to 7 cm (top) and 4 cm (bottom) long. Crystals appear to grow upward by building up successive rosettes, diffusion boundaries exerting control on the growth and shape of crystals, as presently shown by a turbidite layer truncating a vivianite crystal (bottom).